International Journal of Computer Sciences and Engineering Open Access
Research Paper Volume-4, Issue-6 E-ISSN: 2347-2693

A Density Functional Study of Au Clusters Adsorbed on Si(001): Formation of Cluster Lattice and a Transition From Non-Metallicity to Metallicity

Rudra Prasad Bose[1*], Kisalaya Chakrabarti[2]

[1]Birbhum Institute of Engineering & Technology, Suri, Birbhum, West Bengal - 731101, India
[2]Pailan College of Management & Technology,
Bengal Pailan Park, Sector 1, Phase 1, Amgachia Road, Joka, Kolkata -700104, India

www.ijcseonline.org

Received: May/16/2016 Revised: May/30/2016 Accepted: Jun/18/2016 Published: Jun/30/ 2016

Abstract: Electronic structure calculations are carried out under the density functional formalism for understanding the structure and energetic of gold atoms and gold clusters containing up to four atoms adsorbed on the Si(001) surface. The stable adsorption sites of gold atoms and the gold clusters on the Si(001):*p*(2x1) surface and the structural change of the clusters due to their interaction with the surface are presented. Also, the adsorption of Au clusters on Si((001):*p*(2x1) in presence of defects are studied. However, most significant finding of our calculations is that the formation of Au_3 cluster lattice on the Si(001) is possible and, as a consequence, the Si(001) surface becomes metallic.

Keywords: DFS, Au, SET, Atom, Cluster

I. INTRODUCTION

In recent years, there has been tremendous interest in investigating physical and chemical properties of metal clusters in gas phase, as well as those supported on semiconducting substrates[1-8,10,11]. Due to their large surface area to volume ratio, these clusters can be very effective catalysts. Gold clusters are of particular interest because they have promising applications in new nano-devices such as sensors, single electron tunnelling (SET) devices, nano ohmic contacts, nano Schottky contact, heterogeneous catalysis,[12-16] bioelectrocatalysis[17] and photonics[18].

In addition to gas phase metal clusters, ordered metal structures on the silicon surfaces are also of practical importance in silicon microelectronic industry. Consequently, formation of regular arrays of metal clusters on semiconducting substrates has become an interesting area of research. Some important studies[8-10,19-21] of metal clusters on Si surfaces have not only advanced the control of nano fabrication to the ultimate atomic precision, but have also provided a new platform for studying next-generation micro-/nano-electronics such as tuning the Schottky contact, two dimensional (2D) spintronics, surface conductivity and nano catalysis.

It is known that Si(111) and Si(001) are stable surfaces and therefore, these are the surfaces of choice in most of the experiments for examining the possibility of formation of cluster lattices on silicon substrates [19—21]. Before doing such experiments, one needs to understand the interaction of clusters with the substrate along with the interaction among the atoms constituting the cluster. We, therefore carry out electronic structure calculations to understand (i) the energetics and stable adsorption sites of Au atoms and Au_n clusters in the size range "n" = 2-4 on the *p*(2x1) asymmetric Si(001) surface, (ii) structural changes of these clusters due to their interaction with the silicon substrate, (iii) possibility of formation of cluster lattices on Si(001) and (iv) the electrical properties of Si(001) after formation of gold cluster lattice. Our calculations reveal that it is indeed possible to form an Au_3 cluster lattice on Si(001). Finally we conclude that controlled adsorption of Au_3 planer clusters on Si(001): *p*(2x1) may give rise to a smooth metallic surface. Thus we find that the Si(001): *p*(2x1) surface undergoes a non-metallic to metallic transition at a certain coverage of Au_3 clusters.

The paper is organized as follows. The methods of our calculations are discussed in Sec. II. The results and discussions are presented in Sec. III and finally we summarize our findings in Sec. IV.

II. METHOD

All calculations are performed using planewave implementation of the Khon-Sham density functional theory (DFT). The VASP code [22,23] is used for our calculations. The energy cut-off used for plane wave expansion of the wavefunctions is 250 eV. Brillouin Zone integrations are performed using the Monkhorst-Pack scheme[24]. Ionic potentials are represented by projector augmented wave (PAW) potentials. Perdew-Wang (PW91) generalized gradient approximation (GGA) functional is used for the exchange correlation energy. Conjugate gradient is used for ionic relaxation. We use a (2x2x1) k-point mesh for our (4x4) surface super cell. Convergence

with respect to energy cutoff and the number of k-points has been well tested earlier for similar systems [25, 26].

The Si(001) surface is represented by a repeated slab geometry. Each slab contains five Si atomic layers with hydrogen atoms passivating the dangling bonds in the bottom Si layer. Consecutive slabs are separated from each other by 10 Å to avoid any interaction between them. When the clusters are placed perpendicularly on the surface, the slabs are made to separate each other by another 10 Å so that the net separation between consecutive slabs becomes 20Å to avoid any interaction. The Si atoms in the top four atomic layers are allowed to relax, while the bottom layer Si atoms and the H atoms attached to them are kept fixed in order to simulate a bulk-like termination.

Our calculations produce cohesive energy (CE) of a supercell composed of a given set of atoms.

$$E_c[\mathrm{SC}] = E_T[\mathrm{SC}] - E[\mathrm{atoms}] \quad \ldots\ldots (1)$$

Where E_T[SC] is the total energy of the supercell, and E[atoms] is the total energy of all the isolated atoms constituting the supercell. Thus E_c[SC] is the energy gained in assembling the given supercell structure from the isolated atoms. A bound structure, by this definition, has a negative CE.

We call the energy gain in attaching a preformed Au_n cluster to a Si slab as its binding energy (BE) to the surface, which is defined as,

$$E_B = E_T[\text{Si slab}] + E_T[Au_n] - E_T[\text{Si slab} + Au_n] \quad \ldots\ldots (2)$$

where, E_T's are the total energies of the respective systems. Expressing the total energies in terms of the cohesive energies and atomic energies using Eq. 1 it is easy to see that the BE can be written as

$$E_B = E_c[\text{Si slab}] + E_c[Au_n] - E_c[\text{Si slab} + Au_n] \quad \ldots\ldots (3)$$

Where E_c[Au_n] is the cohesive energy of an isolated Au_n cluster. In the latter form, the BE is expressed directly in terms of quantities obtained from our calculations. It should also be noted that the way BE is defined in Eq. 2, it is a positive number if there is an energy gain in attaching an Au_n cluster to a Si surface.

III. RESULTS AND DISCUSSIONS

As we mentioned before, we consider adsorption of an isolated Au atom, and Au_2, Au_3 and Au_4 clusters on the Si(001) surface. Structures of free Au_2, Au_3 and Au_4 clusters are first optimized using VASP. For these and other calculations on isolated clusters or dimers to be discussed later, the cluster under study was placed inside a cubic box of sides 20 Å, and k-point integrations were performed by using the Γ-point only. The results of the optimized structures are as follows. The Au-Au bond length in a Au_2 dimer is 2.76 Å, the Au_3 cluster is found to be an equilateral triangle with a bond length of 2.64 Å and the Au_4 cluster is a rhombus with sides of 2.7 Å. We note that the clusters have planer structures, and our results are in good agreement with results available in the literature[27]. We now systematically present our results on adsorption of a single Au atom and of Au clusters on the Si(001) surface.

A. Isolated Au atom

First we consider adsorption of a single Au atom on the Si(001) surface. There are various special symmetry sites on the Si(001):*p*(2x1) surface[28] for the adsorption of a single Au atom. These are (i) the dimer site (D) on top of the surface Si dimer, (ii) the site vertically above the second layer Si atom and adjacent to surface Si dimer row (M), (iii) the cave site (C) between two surface Si dimers between two dimer rows, and (iv) quasihexagonal site (H) halfway between two surface Si dimers along a dimer row. All these sites are marked (cross symbols) in Fig. 1. Note that all our calculations are done within a 4x4 supercell.

An Au atom was placed at the four special symmetry sites on the surface. Its BE in the final relaxed structure starting from each of these sites is given in Table I. The C site turns out to be the most favourable one for an isolated Au atom with a BE of 3.48 eV. The next favourable sites are H, M and D with binding energies 3.12 eV, 3.10 eV and 2.94 eV respectively. At each of these three sites, the distances between the nearest neighbour Si atoms from the Au atom are in the range 2.42 Å to 2.47 Å. The Au atom initially placed at the C site makes strong bonds with two Si atoms of the adjacent surface Si dimers, and as a result the adjacent Si dimers are stretched by 0.5 Å. In addition, the Au atom at the C site makes weaker bonds with four second layer Si atoms neighbouring it, which are at distances of 3.4-3.5 Å. The Au atom initially placed at the H site moves along the negative of [110] direction, makes strong bonds with two first layer Si atoms in the two

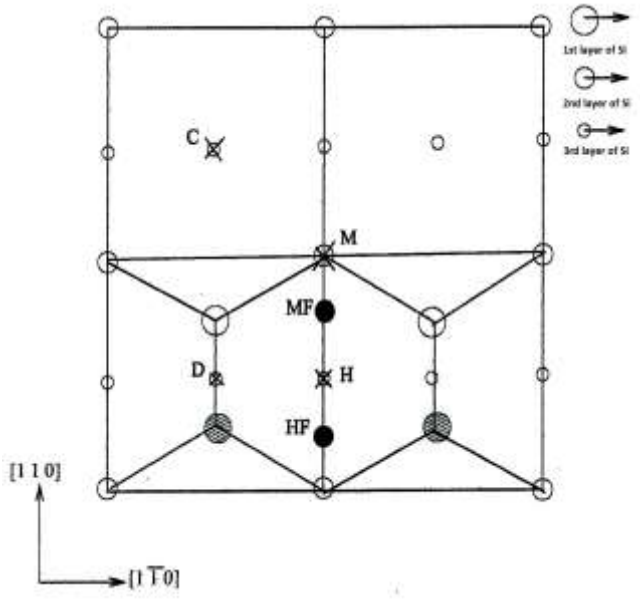

adjacent surface Si dimers, and makes a weak bond with a second layer Si atom which is at a distance of 3Å.

FIG. 1: A schematic diagram of the *p*(2x1) reconstructed Si(001) surface within the 2x2 supercell. The special symmetry sites for adsorption of Au atom and clusters are marked by cross symbols. In the asymmetric surface dimers, the 'up' Si atoms are denoted by the shaded circles.

The Au atom placed at the M site also makes strong bond with two Si atoms of the adjacent Si dimers and a weak bond with a second layer Si atom. Starting from M and H sites, the Au atom ends up in very similar environment in the final relaxed structures. The final positions of the Au atom in these two cases are shown MF and HF in the Fig. 1. This is why the BE's of an Au atom starting from M and H sites are very similar. The C site turns out to be the most favourable one because the Au atom at this site can interact with a large number of neighbouring Si atoms as compared to other symmetry sites. The D site is the least favourable one because at this site an Au atom can make bonds with only two Si atoms in the first layer, and has no second layer Si atoms as neighbour.

TABLE I : BE of Au atom on respective symmetry sites

Positions	Binding Energy (BE) (eV)
C	3.48
H	3.12
M	3.10
D	2.94

B. Au_2 dimer

To understand the adsorption of an Au_2 dimer on the Si(001):*p*(2x1) surface, we place such a dimer with an optimized bond length of 2.76 Å on the surface. A dimer has translational and rotational degrees of freedom and thus, in experimental situations, an incoming Au_2 dimer may move and orient itself to attain the lowest energy configuration on the surface. We, therefore, need to consider different possible orientations of the dimer at different possible orientations of the dimer at different symmetry sites. Earlier studies found that the most favourable orientation of metal dimers on the Si(001) surface is parallel to the surface, being either parallel or orthogonal to the Si dimer rows[29]. However, for the sake of completeness, in addition to such parallel orientations, we also consider initial configurations in which the Au_2 dimers are oriented perpendicular to the surface. In fact, we will see that like other metal dimers, the parallel orientation of Au_2 dimer is energetically more favourable.

For parallel orientation, we consider six different configurations of Au_2 dimer on the surface. These are: (i) parallel to the surface Si dimers with the center of the Au_2 dimer at the H site (Au_2PDH), (ii) orthogonal to the surface Si dimers at the H site (Au_2ODH), (iii) parallel to the surface Si dimers with the center of the Au_2 dimer being above a third layer Si (Au_2PDT), (iv) orthogonal to the Si dimers at the same position (Au_2ODT), (v) parallel to the Si dimers with center at the C site (Au_2PDC), and (vi) orthogonal to the Si dimers at the C site (Au_2ODC). All these initial configurations are shown in Fig.2.

For perpendicular orientation, an Au_2 dimer was placed perpendicular to the surface at the four symmetry sites, namely, C, D, M and H. These are denoted by Au_2pC, Au_2pD, Au_2pM and Au_2pH respectively.

FIG. 2: Initial positions of Au_2 clusters on the symmetry sites.

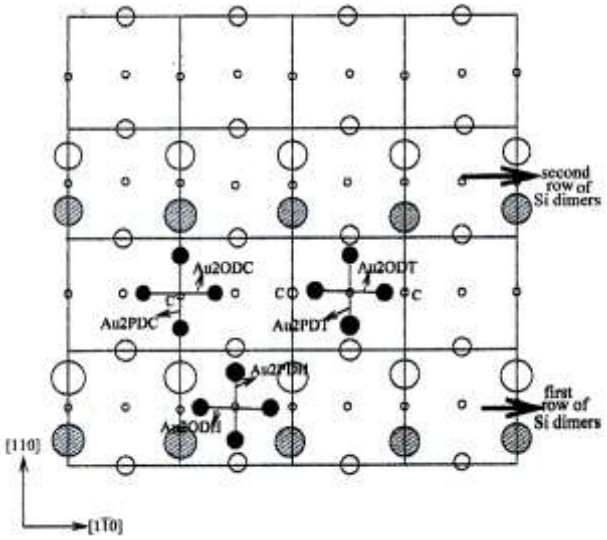

TABLE II: BE of an Au_2 cluster in different configurations on the Si(001) surface. See text for detailed explanation of the configurations.

systems	BE (eV)
Au_2PDC	3.99
Au_2ODC	3.81
Au_2pC	3.99
Au_2pD	2.59
Au_2pM	2.17
Au_2pH	2.17
Au_2PDH	3.81
Au_2PDT	3.19
Au_2ODH	3.35
Au_2ODT	1.73

BEs of an Au_2 dimer in the relaxed structure starting from these ten configurations are given in Table II. The C site again emerges to be the most favourable one and the configuration, Au_2PDC, turns out to be the most stable configuration. In this configuration, the dimer contracts marginally from 2.76 Å to 2.67Å for the two Au atoms to maintain optimal distances from their nearest Si neighbours. In fact, the Au atoms of the dimer are at distances of 2.32 Å and 2.36 Å from their respective nearest neighbour Si atoms on either side (note that the bond length of an isolated Au-Si dimer is 2.36 Å). The BE of an Au_2 dimer at this site is 3.99eV. Interestingly, the Au_2 dimer which was initially placed perpendicular to the surface at the C site (Au_2pC), becomes parallel to the surface and relaxes to the same final configuration as Au_2PDC with the same BE value.

The second most stable configuration is Au_2ODC (see Fig.2.). The binding energy in this case is 3.81 eV. At this

site the Au_2 dimer moves along $[1\bar{1}0]$ direction by 1.85 Å and the dimer bond length becomes 2.97Å from 2.76 Å in order for the two Au atoms to make bonds with two nearest neighbour Si dimers on the first row of Si dimers. The Au-Si distances after relaxation are found to be 2.51Å and 2.45 Å. The Au_2PDH turned out to have the same BE as that of Au_2ODC. During relaxation the Au_2 dimer in the Au_2PDH configuration moves along $[1\bar{1}0]$ direction and make bonds with one of the Si dimer, although initially it has two Si dimers on its either side. Thus, each Au atom makes bond with a single Si atom in the nearest neighbour Si dimer. At this site the Au_2 dimer stretches to a bond length of 2.97Å. In both Au_2PDC and Au_2PDH configurations, each Au atom bonds with one first layer Si atom, but the reason Au_2PDC turns out to be more favourable is that in this configuration, each Au atom has two second layer Si atoms to bond with, whereas in Au_2PDH each Au has only one second layer Si atom.

So far we have considered adsorption of Au_2 cluster on a defect-free Si(001):*p*(2x1) surface. However, most surfaces have defects under experimental conditions, and such defects can have important consequences for nucleation and stabilization of clusters on the surfaces. As an example, defects in the form of Ti-centers on SiO_2 surface have been found to enhance nucleation of Au clusters[30]. Therefore, it is important to ask if it is more favourable for an Au_2 dimer to get adsorbed on a defect-free region of the Si(001) surface, or on a defect. It is well known that missing dimers are a common form of defect on a Si(001):*p*(2x1) surface[31,32]. Therefore, we calculated the BE of an Au_2 dimer in place of a missing Si-Si dimer on this surface. The BE turns out to be 5.27 eV, greater than the BE of an Au_2 dimer on a defect-free surface. Thus it is energetically much more favourable for an Au_2 dimer to bind in place of a missing surface Si dimer than in a defect-free region, and we can expect that such missing surface dimers will play a major role in adsorption and dynamics of Au clusters on the surface.

As we will show, energetics of Au clusters on the Si(001) surface can be understood in terms of the relative strengths of Au-Au, Au-Si and Si-Si bonds. We calculated CEs of free standing Au_2, Au-Si, and Si_2 dimers with the same methods used to study the Si(001) surface. The CE of an Au-Si dimer turned out to be -4.14 eV, whereas an Au-Au bond has a much lower cohesive energy of -2.65 eV. The CE of free standing Si_2 dimer is -4.65 eV. This clearly shows that there is an energy gain in forming Au-Si bonds even at the cost of Au-Au bonds. While Au-Au and Au-Si bond strengths will be different on the Si(001) surface compared to free dimers, these values can be used as guides to arrive at a qualitative understanding of the observed behaviour.

Using the information that there is a large energy gain in forming an Au-Si dimer, one can easily rationalize the energy orderings of the four special symmetry sites for adsorption of an isolated Au atom. The energy orderings of these sites are in order of the number of Au-Si bonds that can be formed, as we have already indicated. This also explains why Au_2 dimers prefer to be adsorbed parallel to the Si(001) surface, rather than being perpendicular to it. Being parallel to the surface, both the Au atoms can form bonds with Si atoms, while in the perpendicular orientation; one of them cannot do so. For adsorption of Au_2, Au_2PDC turns out to be the most favourable because in this configuration, the Au atoms can form optimal bonds with one first layer Si atom each, while they can also bond with two second layer Si atoms each. The Au atoms also maintain the bond between them. This leads to a large gain in energy. In Au_2ODC, each Au atom makes comparatively weaker bonds with two first layer Si atoms each. Thus this configuration has a slightly lower BE of 3.81 eV. The least favourable configuration turns out to be Au_2ODT with BE ~ 1.72 eV. In this configuration the Au_2 dimer breaks, and Au-Au distance increases from 2.76Å to 3.72Å. Both the Au atoms move in the [110] direction to make bonds with the first layer Si atoms of the second row of dimers. But in the final configuration, they form bonds with only one first layer and one second layer Si atom each. This small number of Au-Si bonds, and the fact that the Au-Au bond is broken, leads to an energy gain of only 1.72 eV.

One of the most commonly used experimental probes to study surface structures is scanning tunnelling microscope (STM). Although STM images are often used to study atomic structures of surfaces, or adsorbents on substrates, what STM really measures is a complicated convolution of the surface and tip electronic states. Therefore, it is crucial to understand if the observed electronic structure of the Si(001) supported Au clusters would allow us an atomic resolution of the cluster structure. In fact, Walter et al.[33] have shown using similar DFT methods that STM images cannot resolve atomic structure of small Au clusters supported on MgO surface due to the delocalized nature of the cluster electronic states originating from the s states on the Au atoms. We have done a somewhat similar, but simpler analysis using ideas from the work of Tersoff and Hamann[34]. What we plot in Fig. 3 are charge density contours in a plane 2Å above the Au_2 dimer in the final configuration of Au_2PDC coming from states (occupied for the filled state image, and unoccupied for the vacant state image) within a range of 1eV of the Fermi energy. This is a qualitative indication of what one can expect in an STM experiment if the tip height was kept fixed and a bias of 1eV was applied. As seen from this simulated images, an area larger than the atomic structure of the dimer has a large uniform charge distribution. This suggests that an STM will not be able to resolve the atomic structure of the adsorbed Au_2 dimer.

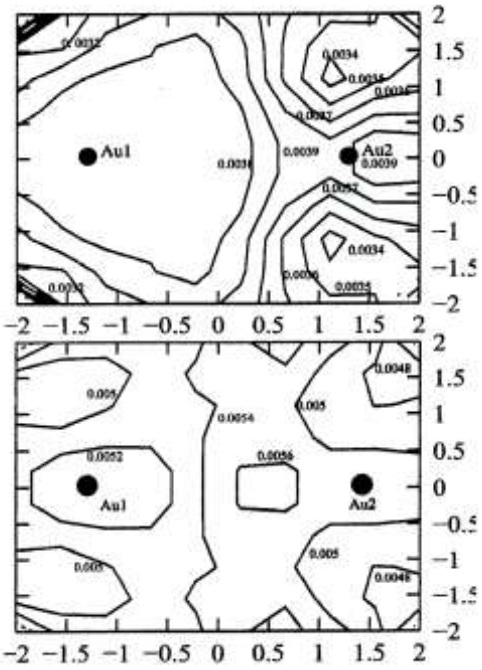

FIG.3: Qualitative simulated vacant state (top) and filled state (bottom) STM image of Au_2 cluster on the most favourable C site.

C. Au_3 cluster

In order to study adsorption of Au_3 clusters, all shapes of Au_3 cluster was studied such as linear, acute angle triangle, obtuse angle triangle, right angle triangle, L shaped and other configurations, but the most stable and optimized structure we obtained is an equilateral triangle with side 2.64Å. We placed an optimized triangular Au_3 cluster at different positions on a (4x4) surface supercell of the Si(001) surface. In this case also we chose two orientations of the cluster with respect to the surface: the plane of the triangle being parallel or perpendicular to the surface. While placing the cluster parallel to the surface, we choose the following configurations: one side of the equilateral triangle kept parallel to a surface Si dimer and the center of the triangle made to coincide with either (i) an H site (Au_3PH) or (ii) a C site (Au_3PC); one side of the triangle is oriented orthogonal to a surface Si dimer and the center of the triangle is placed (iii) at an H site (Au_3OH) or (iv) at a C site (Au_3OC) (v) one side of the equilateral triangle is oriented orthogonal to a surface Si dimer with its center coinciding an M site (Au_3OM). All this initial configurations are shown in Fig. 4. We further chose four configurations in case of perpendicular orientation: One side of the triangle is parallel to a surface Si dimer with the center of the side (i) at an H site (Au_3PHp) or (ii) at a C (Au_3PCp) site; and one side of the triangle orthogonal to a surface Si dimer with its center again (iii) at a H (Au_3OHp) or (iv) at a C (Au_3OCp) site.

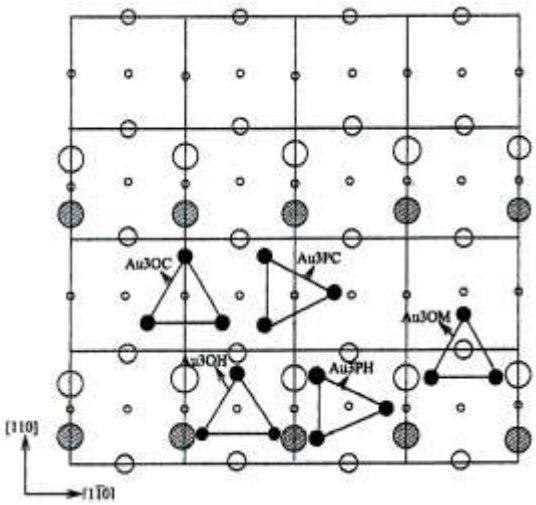

FIG. 4: Initial positions of Au_3 cluster on the symmetry sites of p(2x1) reconstructed Si(001) surface.

TABLE III: BE of an Au_3 cluster on symmetry sites of a p(2x1) reconstructed Si(001) surface

systems	BE(eV)
Au_3PC	5.74
Au_3PH	5.65
Au_3OH	5.59
Au_3OM	5.59
Au_3OC	4.66
Au_3PCp	5.17
Au_3OHp	5.05
Au_3PHp	4.48
Au_3OCp	3.85

The BEs for all these configurations are given in the Table III. We find that the Au_3PC configuration turns out to be the most favourable one with a BE of 5.74 eV. The second and the third best configurations, as seen from the table III, are Au_3PH and Au_3OH with BE of 5.65 eV and 5.59 eV respectively. All the three configurations, however, are very close in their BE values. The reason for the C site being most favourable is that the Au_3 cluster at this site has more neighbouring Si atoms to interact with. The final converged structures for these initial configurations are shown in Fig. 5. In case of Au_3PC the Au-Au bond lengths are stretched slightly. Referring to Fig. 5, the altered distances between Au_1-Au_2 is 2.97 Å. The distance between Au_1 and Au_3 is 2.72Å, and the distance between Au_2 and Au_3 is 2.78Å. The Au atoms of the Au_3 cluster at the C site make strong bonds with the neighbouring Si atoms with bond lengths ranging from 2.35Å to 2.39Å.

In the final structure of Au_3PH, two of the Au-Au bonds stretch to 2.81 Å, and the third bond is almost broken with an Au-Au distance of 3.42Å, as shown by a dashed line in Fig. 5. In Au_3OH one of the Au-Au bonds is stretched to 2.87Å, and two Au-Au bonds are stretched to 3.06Å from their gas phase optimized bond length of 2.64Å. Thus in the last two cases, the Au_3 clusters tend to break up and the Au atoms move towards the nearest

neighbour Si atoms to make strong bonds with them. This is again consistent with the fact that an Au-Si bond is stronger than an Au-Au bond.

The perpendicular configurations were relatively less stable. This is understandable as one of the Au atoms cannot make bonds with Si atoms in these configurations. In fact, in the
final structures of Au_3OHp and Au_3OCp, the Au_3 triangle tilts from the initial perpendicular position, so that the apical Au atom can make bonds with the surface Si atoms. In configurations Au_3PCp and Au_3PHp the Au_3 triangle remains in the perpendicular position with the bond length between the bases Au atoms increasing from 2.64Å to 2.87Å, and 3.13Å respectively. Among the perpendicular orientations, Au_3PCp and Au_3OHp have higher BE values because in these configurations Au atoms have a larger number of nearest neighbour Si atoms. Even though the Au_3 triangle tilts and the apical Au atom tries to make bonds with the Si atom in the Au_3OCp configuration, it turns out to have the least BE. This is because the distances from the apical Au to its nearest neighbour Si atoms are still quite large: 2.7-2.9Å from first layer Si atoms and 3.5-3.6Å from second layer Si atoms. These are much larger than their optimum Au-Si bond length of 2.36Å. In addition, the base Au-Au bond of the Au_3 cluster stretches from 2.64 Å to 2.8Å.

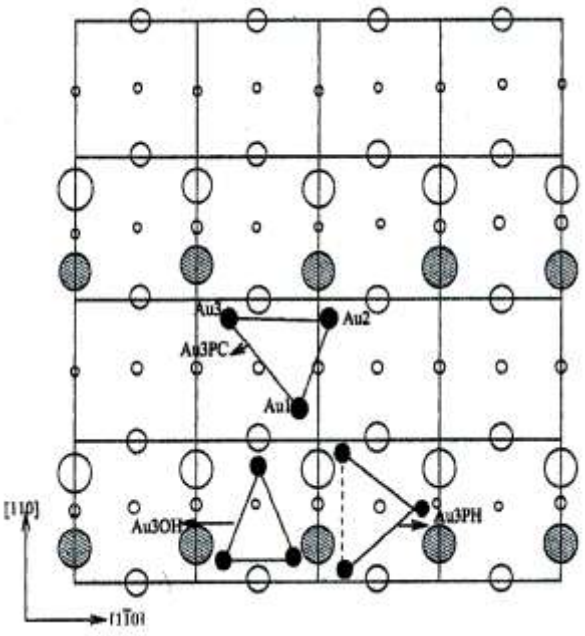

FIG.5: Final position of Au_3 cluster on the first three most favourable sites.

To understand if the atomic resolution of the structure of an Au_3
cluster on the substrate is possible or not in STM experiments, we have produced the simulated vacant and filled state STM images for the final structure of Au_3PC, and it is shown in the Fig. 6. As in the case of Au_2 dimer, the charge density is found to be uniformly high over an area larger than the size of the Au_3 cluster. Therefore, STM experiments will not be able to resolve atomic structure of an Au_3 cluster adsorbed on the Si(001) surface.

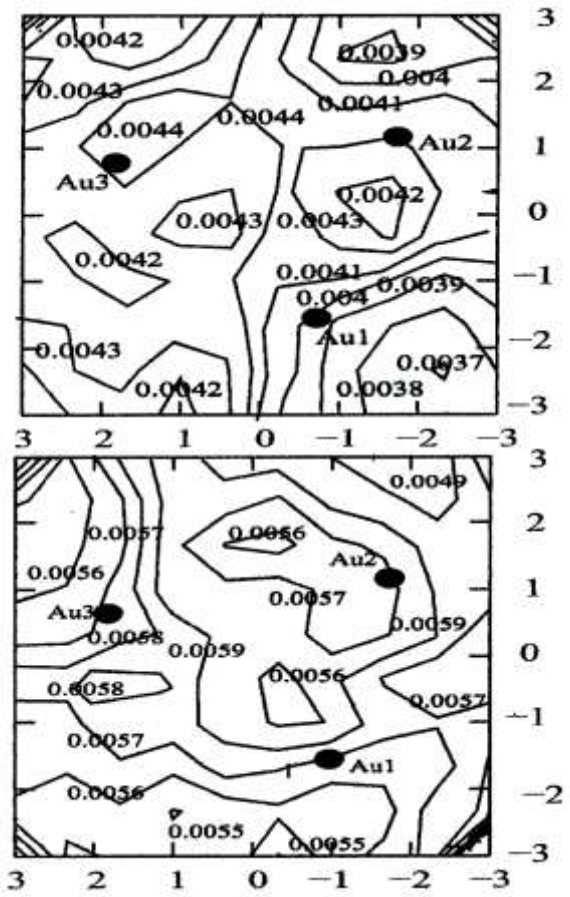

FIG.6: Filled state STM image (top) and vacant state STM image (bottom) of Au_3PC cluster configuration on the most favourable C site.

To have an idea about the effect of missing dimer defects on the adsorption of Au_3 clusters on the surface, we placed an Au_3 cluster at the site of a missing surface Si dimer in two orientations: one side of the Au_3 cluster occupying the missing dimer position and (i) the third atom vertically above, so that the Au_3 triangle is perpendicular to the surface and (ii) the third atom also in a plane parallel to the Si(001) surface, i.e., the whole triangle is parallel to the surface. Both the configurations converge to the same relaxed structure with a BE ~ 6.7 eV, which is higher than BE's for adsorption of Au_3 clusters on a defect-free Si(001) surface. Thus, it is energetically much more favourable for an Au_3 cluster to bind in place of a missing surface Si dimer than on a defect-free region of the Si(001) surface.

D. Au_4 cluster

As previously stated, we have studied different shapes of Au_4 cluster for example. linear structure, T-shaped structure, square, rectangular, parallelogram and trapezoid structures in 2D configurations and tetrahedral and other 3D structures but the optimum structure obtained for an Au_4 cluster is a rhombus with an Au-Au bond length of 2.7Å. In order to study adsorption of Au_4 on the Si(001)

surface, we placed an optimized Au_4 cluster, with its center at an H or a C site, in two different configurations : (i) the larger diagonal of the rhombus is parallel to surface Si dimers (Au_4PC and Au_4PH), (ii) the larger diagonal is perpendicular to the Si dimers (Au_4OC and Au_4OH). These initial configurations are shown in Fig. 7, and the BEs of the final relaxed structures is given in Table IV.

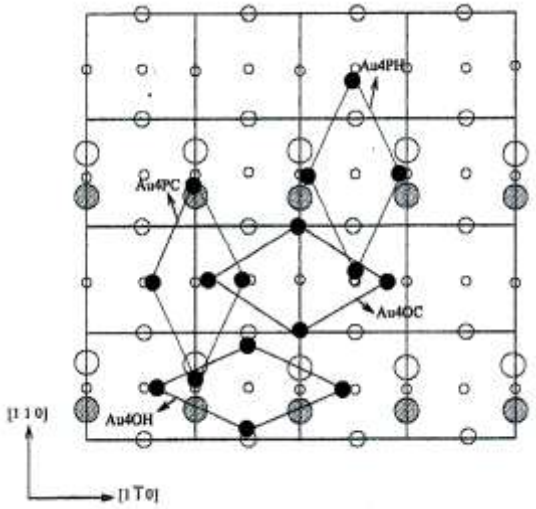

FIG.7: Initial positions of the Au_4 cluster on the symmetry sites.

The relaxed configurations, Au_4OC turned out to be the most favourable one for an Au_4 cluster with a BE of 6.27 eV. In the initial structure, the four Au atoms had their nearest neighbour Si atoms at distances of 3.31, 2.88, 2.31 and 3.37Å respectively.

TABLE IV: BE of Au_4 cluster on respective symmetry sites

systems	BE (eV)
Au_4OC	6.27
Au_4PC	6.06
Au_4OH	5.46
Au_4PH	4.90

However, after relaxation, the Au_4 cluster breaks up and each Au atom tends to form optimal bonds with its nearest surface Si atom. This can be clearly seen in Fig. 8, where the nearest neighbour Au-Si distances are 2.35Å (from Au_1), 2.33Å (from Au_2), 2.41Å (from Au_3) and 2.34Å (from Au_4) respectively. Thus the Au atoms form strong bonds with surface Si atoms even at the cost of breaking up the structural identity of the Au_4 cluster.

In the other three configurations, the BE is lower than that of Au_4OC, but the Au_4 cluster retains its structural identity. The second highest BE, as seen from the Table IV, is in the case of Au_4PC with a value of 6.06 eV. Here the bonds between the Au atoms stretch from their optimum value of 2.7Å to an average of 3Å. The Au_4 cluster also moves by 2Å along the [110] direction. In Au_4PH and Au_4OH, the rhombus is stretched along the short diagonal and is compressed along the long diagonal. In Au_4PH the Au-Au bond length remains unchanged at its gas-phase values, while in Au_4OH it is marginally stretched from 2.7Å to 2.8Å. We therefore conclude that depending on adsorption site, an Au_4 cluster may lose its identity on the Si(001) surface.

On viewing this we tried to observe the dynamics of Au_3 and Au_4 clusters on the surface. That is we have placed defragmented Au_3 and Au_4 clusters at different symmetry sites and other sites, but their accumulated energy occurs to be less than the BE of Au_3PC but almost equal to Au_4OC. Hence we confirm that cluster lattice cannot be formed with Au_4 cluster but with Au_3 cluster there is a great possibility of forming cluster lattice. With this information we proceed in the following section about the formation of a possible cluster lattice.

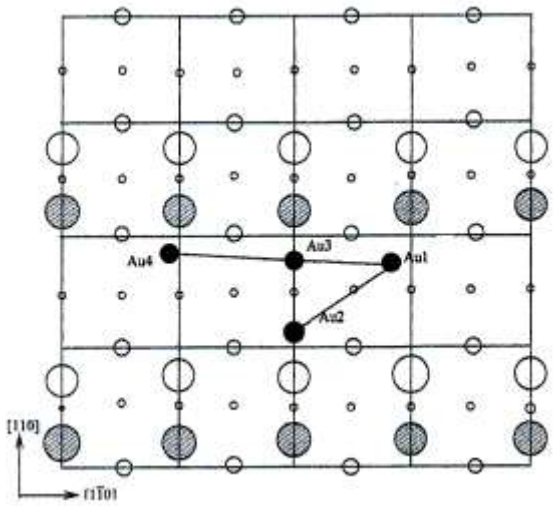

FIG.8: Au_4 cluster on the most favourable C site.

In the final structure of Au_4OC, the calculated STM image shows a large charge density over a region larger than the size of the Au_4 (though disintegrated) cluster, thus indicating that it will not be possible to understand the atomic structure from such an image. The filled and vacant state images are shown in Fig. 9.

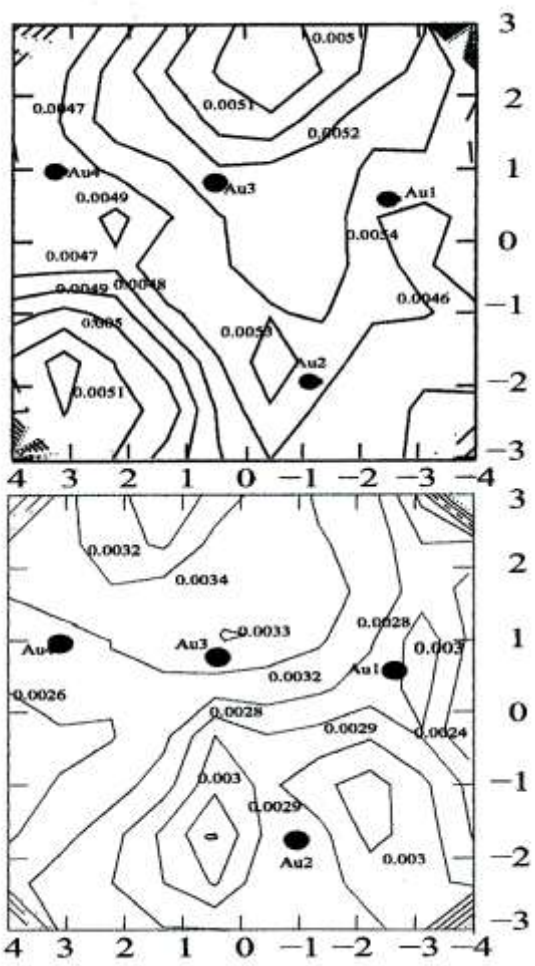

FIG.9: Qualitative simulated filled state (top) and vacant state (bottom) STM image of Au_4 cluster on the C site.

E. Arrays of Au_3 clusters

Finally we explore the possibility of formation of an array of gold clusters on the Si(001):*p*(2x1) surface. Our adsorption studies of Au_3 and Au_4 clusters on Si(001) already indicated that an Au_4 cluster disintegrates due to its interaction with the surface Si atoms, while an Au_3 cluster, in its most favourable configuration, retains its structural identity. We therefore, consider Au_3 clusters as building blocks for the possible formation of a cluster lattice on the Si(001) surface. The relaxed configuration of an Au_3 cluster at the most stable C site (see Sec.IIIC) is considered for this purpose. Here we have used the (4x4) super cell of the Si(001):*p*(2x1). Note that there are a total of eight C sites within the (4x4) super cell. With one Au_3 cluster at a C site, we find that a second Au_3 cluster also prefers to bind at either the nearest neighbour C site (along [110]) or the next nearest neighbour C site (along$[1\bar{1}0]$) available in the 4x4 supercell. Moreover, the total BE of the two Au_3 dimers is independent of where the second Au_3 cluster binds, and the value is 5.89 eV per Au_3. Therefore, the final configuration after the adsorption of two Au_3 clusters turns out to be cluster rows extending along either $[1\bar{1}0]$ or [110]. The BE per cluster in this case is larger than that when a single Au_3 cluster is adsorbed within the 4x4 super cell, possibly due to a weak cluster-cluster interaction. However, a plot of band structure (not shown for brevity) shows that this surface still remains semiconducting.

We next put two more Au_3 clusters on the Si(001) surface so that there are a total of four Au_3 clusters in a (4x4) super cell. (see Fig. 10). Apart from the configuration shown in the Fig. 10, we also considered various other configurations. It turns out that the configuration with four Au_3 clusters occupying four C sites as in Fig. 10 is the most favourable one with a BE of 5.81 eV per Au_3. The relaxed atomic structure of Au_3 cluster lattice on the Si(001) :*p*(2x1) surface is shown in the Fig. 11. For this configuration, we have plotted the band structure and the corresponding density of states in Fig. 12. The band structure plot clearly shows bands crossing the Fermi level. This is reflected in the DOS (right panel of Fig. 12) which is finite at the Fermi level. Thus, the Si(001):*p*(2x1) surface becomes metallic in nature due to the formation of a lattice of Au_3 clusters. Hence, we come to the very important conclusion that the Si(001):*p*(2x1) surface undergoes a non-metallic to metallic transition at a certain coverage of Au_3 clusters. We, therefore, propose that experiments in this direction may be designed to obtain a smooth metallic Si(001) surface for technological applications.

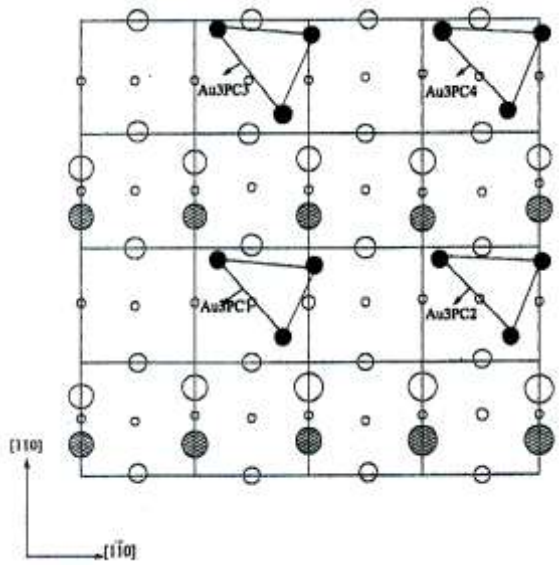

FIG.10: Schematic diagram of the four Au_3 clusters on all the four symmetric C sites within the (4x4) supercell of the Si(001): *p*(2x1) surface.

IV. CONCLUSIONS

We have studied the energetics of single Au atom, Au_2 cluster, Au_3 cluster and Au_4 cluster adsorbed on the clean *p*(2x1) reconstructed Si(001) surface within the density functional formalism. We find that Au_2, Au_3 clusters on the Si(001) surface retains its identity as clusters while the Au_4 cluster on the Si(001) surface breaks into fragments. The effect of missing Si dimers on the adsorption of Au clusters are studied and it is found that

the clusters prefer to bind at the missing Si dimer locations on the Si(001) surface.

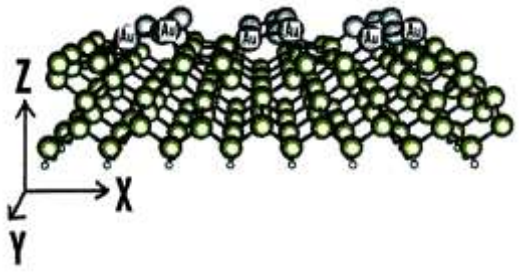

FIG.11: Relaxed atomic structure of Au_3 cluster lattice on Si(001):*p*(2x1) surface. The X, Y and Z directions correspond to [110], [1$\bar{1}$0] and [001] respectively.

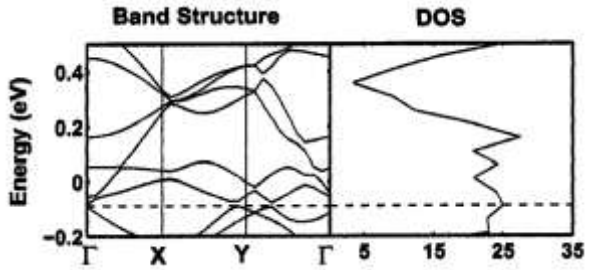

FIG.12: Density of states of Si(001) when four Au_3 clusters are adsorbed within the (4x4) supercell of Si(001):*p*((2x1) surface (see right panel). The band structure plot of the same system is shown in the left panel. Both the plot indicate that the Si(001):*p*(2x1) surface becomes metallic due to the adsorption of four Au_3 clusters within the (4x4) supercell.

Based on the results of the adsorption of isolated clusters on clean Si(001):*p*(2x1) surface we have studied the possibility of the formation of Au_3 cluster lattices. Our calculation reveals that formation of stable Au_3 cluster lattice is indeed possible on the clean Si(001) :*p*(2x1) surface. Most interestingly, at certain coverage of Au_3 clusters, the Si surface turns metallic. We therefore, propose that Au_3 cluster adsorption experiments may be designed to obtain a metallic Si(001) surface that can have useful applications in the electronics industry.

Acknowledgements

Rudra. P. Bose acknowledges the partial financial support from the CSIR sponsored project: 03(1081)06EMR-II. In addition, Rudra P. Bose acknowledges the support provided by H.R.I., Allahabad. All the computations are carried out at the cluster computing facility in H.R.I. Allahabad.

Conflict of Interest

The authors declare that there is no conflict of interest regarding the publication of this manuscript.

References

1. J. L. Li, J. F. Jia, X. J. Liang, X. Liu, J.Z. Wang, Q. K. Xue, Z. Q. Li, J.S. Tse, Z. Zhang, and S. B. Zhang, Phys. Rev. Lett. **88**, 066101 (2002).
2. J.F. Jia, X. Liu, J.Z. Wang, J. L .Li, X. S. Wang, Q. K. Xue, Z. Q. Li, Z. Zhang, and S. B. Zhang, Phys. Rev. B **66**, 165412 (2002).
3. Kehui Wu, Y. Fujikawa, T. Nagao, et al, Phys. Rev. Lett. **91**, 126101 (2003).
4. Shao Chun Li, Jin Feng Jia, Rui Fen Dou, et al, Phys. Rev. Lett., **93**, 116103 (2004).
5. J. Jia, Jun Zhong Wang, et al Appl. Phys. Lett. **80,** 3186 (2002).
6. M. Y. Lai and Y.L. Wang, Phys. Rev. B, **64,** 241404(R)2001).
7. H. H. Chang, M. Y. Lai, et al, Phys. Rev. Lett., **92**, 066103 (2003).
8. J. R. Ahn, J. H. Byun, W. H. Choi, H. W. Yeom, Phys. Rev. B, **70**, 113304 (2004).
9. J.M. Zuo and B. Q. Li, Phys. Rev. Lett. **88**, 255502 (2002).
10. V. G. Kotlyar, A. V. Zotov, A. A. Saranin, et al, Phys. Rev. B **66**, 165401 (2002).
11. Saroj. K. Nayak and P. Jena, et al Phys. Rev. B **56**, 6952 (1997).
12. B. Gates, Chem. Rev. (Washington D. C.) **95**, 511 (1995).
13. M. Haruta, Catal. Today **36**, 153 (1997).
14. G. Bond and D. Thompson, Catal. Rev. Sci. and Eng. **41**, 319 (1999).
15. R. Meyer, C. Lemire, S. K. Shaikhutdinov, and H. Freud, Gold Bull. **37,** 72 (2004).
16. C. R. Henry, Prog. Surf. Sci., **80,** 92 (2005).
17. Y. Xiao, F. Patolsky, E. Katz, et al, Science **299**, 1877 (2003).
18. W. L. Barnes, A. Dereux, and T. W. Ebbesen, Nature (London). **424**, 824 (2003).
19. Dinesh Kumar Vankatachalam, Dinesh Kumar Sood and Suresh Kumar Bhargava, Nanotechnology **19**, 015605 (2008)
20. Lixin Zhang, S. B. Zhang, Qi-Kun Xue, Jin-Feng Jia and E. G. Wang, Phys. Rev. B. **72**, 033315 (2005).
21. Ivan Ost'adal, Pavel Kocan, Pavel Sobotik and Jan Pudl, Phys. Rev. Lett. **95**, 146101 (2005).
22. G. Kresse and J. Furthmuller, Phys. Rev. B **54,** 11169 (1996).
23. G. Kresse and J. Hafner, Phys. Rev. B **47**, 558 (1993).
24. H. J. Monkhorst and J. D. Pack, Phys. Rev. B, **13**, 5118 (1976).
25. P. Sen, S. Ciraci, I. P. Batra and C. H. Grein, Phys. Rev. B **64**, 193310 (2001).
26. A. J. Ciani, P. Sen, and I. P. Batra, Phys. Rev. B **69**, 245308 (2004).
27. Jin Zhao, Jinglong Yang, and J. G. Hou, Phys. Rev. B **67**, 085404 (2003).
28. P. Sen, B. C. Gupta and I. P. Batra, Phys. Rev. B **73**, 085319 (2006) .
29. B. C. Gupta and I. P. Batra, Phys. Rev. B, **69**, 165322, (2004).
30. W. T**.** Wallace, B. K. Min and D. W. Goodman, Jl Mol. Cat. A: Chem **228**, 3 (2005).
31. E. Kim, C. Chen, T. Pang, and Y. H. Lee, Phys. Rev. B **60**, 8680 (1999).
32. M. H. Tasi, Y. Tasi, C. S. Chang, Y. Wei, and I. Tsang, Phys Rev. B **56**, 7435 (1997).
33. Michael Walter, Pentti Frondelius, Karolina Honkala, Hannu Hakkinen, Phys. Rev. Lett. **99**, 096102 (2007).
34. J. Tersoff and D. R Hamann, Phys. Rev. Lett. **50**, 1998 (1983).

